stellarator news

Published by Fusion Energy Division, Oak Ridge National Laboratory
Building 9201-2; P.O. Box 2009; Oak Ridge, TN 37831-8071, USA
Editor: James A. Rome
Issue #26
March 1993
E-Mail: jar@ornl.gov
Phone: (615) 574-1306

Around the Labs

Magnetic island studies on CAT

Over the past year, the study of magnetic islands has been the primary focus of research on the Compact Auburn Torsatron (CAT) at Auburn University, Alabama. With two main helical windings ($l = 2$, $m = 5$ and $l = 1$, $m = 5$), we can change CAT's rotational transform profile to access various magnetic islands. Most of the magnetic island studies have dealt with reducing the size of the $\iota = 1/2$ island.

Initially, a pair of Helmholtz coils producing orthogonal, horizontal magnetic fields was placed on CAT [1]. By sweeping the currents in the Helmholtz coils we were able to determine the correct magnitude and direction of the applied horizontal field to minimize the extent of the $\iota = 1/2$ magnetic island. Fig. 1 is a plot of the O-point width of the $\iota = 1/2$ island as a function of the current in one of the Helmholtz coils. From Fig. 1, it can be seen that the width of the magnetic island has been considerably reduced.

One of the most important things that we learned from the Helmholtz coil studies is that the poloidal phase of the magnetic island (measured as the poloidal location of the O-points) should be kept constant when studying the magnetic island. It has been found that if the direction of the imposed correction field is kept constant and along the direction of the inherent error field causing the magnetic island, then the poloidal phase will be constant (except for an approximate $\pi/2$ rotation as the value of the correction field passes through the value of the error field).

We have also placed a set of helical correction coils $l = 2$, $m = 1$) on CAT to interact more efficiently with the $\iota = 1/2$ magnetic island. Results show that the currents necessary to minimize the island size are substantially less than the currents needed in the Helmholtz coils. Fig. 2 shows the O-point width of the magnetic island as a function of the currents in the helical 1/2 coils.

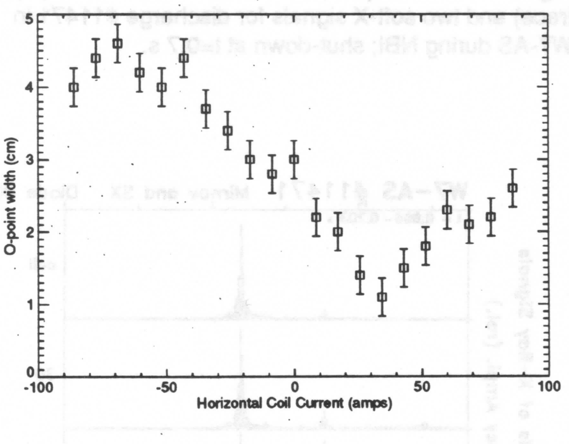

Fig. 1. O-point width vs current for $\iota = 1/2$ islands. For this plot, the correction fields were produced by the Helmholtz coils.

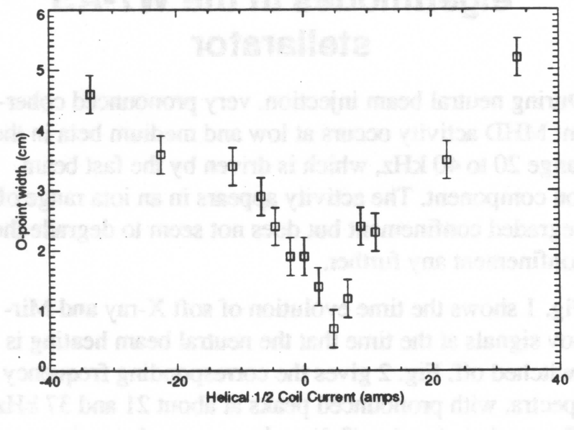

Fig. 2. O-point width vs current for $\iota = 1/2$ islands. Here, the correction fields were produced by the helical 1/2 coils.

Magnetic islands have been theoretically described using Hamiltonian theory [2], with the formalism similar to that of a simple pendulum. Currently, we are investigating methods to describe the global behavior of the magnetic islands by measuring the local rotational transform profiles of the interior magnetic flux surfaces bounded by the separatrix surface. With this method we measure the island size by determining the local rotational transform at the O-point of the island, λ_0, which is analogous to the rotational transform at the magnetic axis, ι_0. We are also working on methods to experimentally validate the Hamiltonian description of the magnetic islands.

Gregory J. Hartwell for the CAT Group
Department of Physics
206 Allison Lab
Auburn University
Auburn, AL 36849 USA

Phone: 205-844-2358
Internet: hartwell@torsatron.nsrc.auburn.edu

REFERENCES

[1] C. B. Brooks et al., Nuclear Fusion 32, No. 11, 2001 (1992).
[2] J. R. Cary and J. D. Hanson, Phys. Fluids B3, 1006 (1991).

Neutral-beam-driven Alfvén eigenmodes in the W7-AS stellarator

During neutral beam injection, very pronounced coherent MHD activity occurs at low and medium beta in the range 20 to 40 kHz, which is driven by the fast beam ion component. The activity appears in an iota range of degraded confinement but does not seem to degrade the confinement any further.

Fig. 1 shows the time evolution of soft X-ray and Mirnov signals at the time that the neutral beam heating is switched off. Fig. 2 gives the corresponding frequency spectra, with pronounced peaks at about 21 and 37 kHz. The mode is $(m,n) = (3,1)$ and corresponds to ι just above 1/3 at a field $B = 2.5$ T. NBI with a power of 400 kW in co-injection is applied to a currentless plasma of an average density $n_e = 5.5\ 10^{13}\ \mathrm{cm}^{-3}$.

These modes are discussed in terms of marginally stable global Alfvén eigenmodes (GAE), which are destabilized by beam-wave resonances of the fast circulating particles. GAE modes are discrete global modes in gaps below the shear-Alfvén continua. They are weakly damped in W7-AS because the toroidal coupling to the shear-Alfvén continua is weak. This is due to low shear and large aspect ratio. The gaps of low (m,n) continua are generated in W7-AS, because low-order rational values of the rotational transform $\iota = 1/q = n/m$ are normally excluded from the confinement region. Toroidal Alfvén modes (TAE) have been seen in tokamaks and cause losses of fast particles. TAEs are caused by toroidal coupling between adjacent poloidal mode numbers m and $m+1$, at identical toroidal mode number n, inside toroidicity-induced gaps of the Alfvén spectrum.

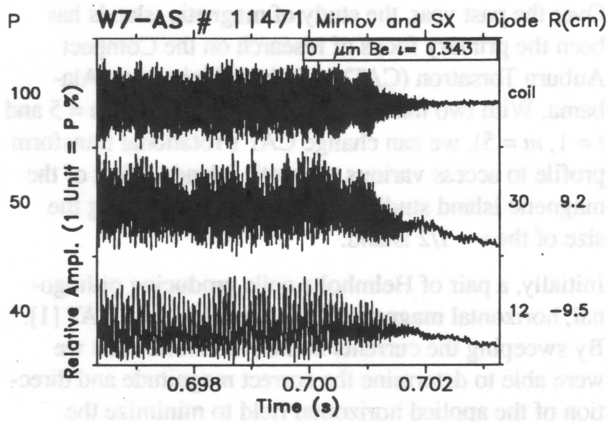

Fig. 1. Relative amplitudes of Mirnov-oscillations (top trace) and two soft-X signals for discharge #11471 in W7-AS during NBI; shut-down at t=0.7 s.

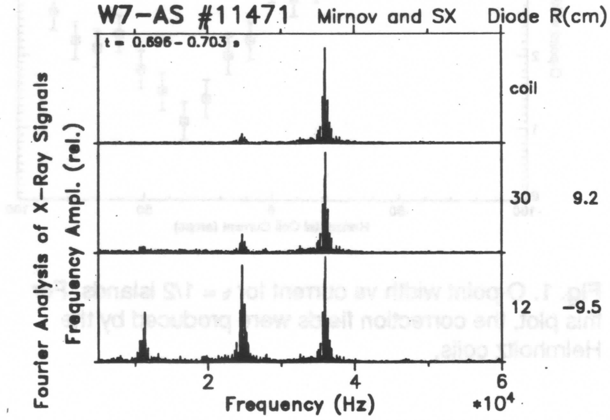

Fig. 2. Frequency spectrum corresponding to the signals of Fig. 1.

In W7-AS, however, TAEs with low (m,n) are not expected because of the flat iota profile. The expected frequencies of the (3,1) and (5,2) shear-Alfvén continua are shown in the top part of Fig. 3, with reference to the data of the previous figures. Experimentally deduced profiles of density (bottom part) have been used to calculate the Alfvén velocity profile, and of iota (middle part) to calculate the parallel wave number $k_{\|}$. The horizontal bars show the GAE frequency (at about 23 and 90 kHz), predicted by a simplified analytical calculation. The radial range marked by the bars gives an estimate of where beam wave resonances are expected to take place.

In summary, A number of experimental observations suggest the interpretation of the experimental observations with global Alfvén modes:

➡ The injected particle velocity is on the order of the Alfvén velocity.

➡ The observed frequencies and poloidal mode numbers and the particle resonance conditions are consistent with global Alfvén wave predictions (dependence on B, n_e, $\iota(a)$, co/ctr NBI).

➡ The observed frequencies scale roughly linearly with the mean Alfvén velocity under various conditions.

➡ The modes switch off with NBI much faster than the slowing-down time.

➡ The poloidal rotation is always in the direction of the diamagnetic drift of the fast ions.

➡ Estimates with analytic expressions for the growth rate show that the driving terms can exceed electron Landau damping, especially in the case of a sufficiently steep fast-ion density gradient.

➡ If low-frequency, pressure-driven modes are present simultaneously (rotating in the opposite direction), beam-driven modes of the same mode number are "forbidden" (no gap, continuum damping).

➡ First stability calculations for GAEs in W7-AS have been made with a reduced MHD model, which includes the fast particles by a gyrofluid description [1]. This Oak Ridge code has been successfully applied to model TAE modes in DIII-D and TFTR. The initial results (linear growth rate, frequency, mode structure, and nonlinear saturation levels) fit the experimental data of W7-AS quite well.

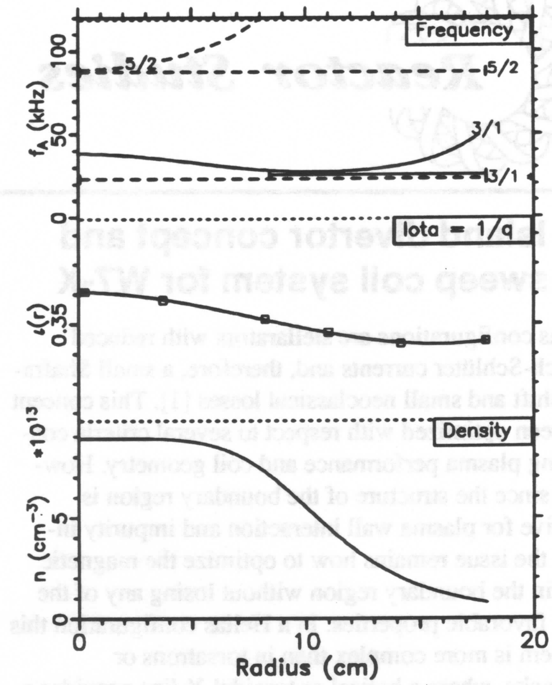

Fig. 3. Radial profiles for the shear-Alfvén continua with mode numbers (3,1) and (5,2) and radial range of beam-wave resonances (solid/dashed line for co/counter injection) (*top*), and deduced from the experimental data of iota and density, (*middle* and *bottom*).

REFERENCES

[1] D. A. Spong, B. A. Carreras, and C. L. Hedrick, Phys. Fluids B4, 3316 (1992).

Arthur Weller, W7-AS Team, NBI Group
Max Planck Institut für Plasmaphysik
Experimental Division E3A
D-8046 Garching bei München, Germany
Phone: 049-89-3299-1905
FAX: 049-89-3299-2584

and

Donald A. Spong
Oak Ridge National Laboratory
P.O. Box 2009, Oak Ridge, TN 37831-8071 USA
Phone: (615) 574-1304
FAX: (615) 576-7926

Reactor Studies

Island divertor concept and sweep coil system for W7-X

Helias configurations are stellarators with reduced Pfirsch-Schlüter currents and, therefore, a small Shafranov shift and small neoclassical losses [1]. This concept has been optimized with respect to several criteria concerning plasma performance and coil geometry. However, since the structure of the boundary region is decisive for plasma wall interaction and impurity inflow, the issue remains how to optimize the magnetic field in the boundary region without losing any of the other favorable properties. In a Helias configuration this problem is more complex than in torsatrons or tokamaks, where a helical or toroidal X-line provides a rapid diversion of field lines. In the Helias configuration two options for a divertor configuration exist, these are an ergodic divertor or an island divertor; both are being studied.

Ergodic divertor

In an ergodic divertor configuration, the last magnetic surface is surrounded by an ergodic layer without large magnetic islands. Plasma losses occur mainly along the helical edge, where field line diversion is at its maximum. The target plates follow the helical edge and are appropriately shaped to minimize the local wall load (in the helical trough). This concept is rather insensitive to changes of the rotational transform and therefore well suited to an experiment where, for the sake of experimental flexibility, the transform may be varied. Studies on the ergodic divertor in Helias configurations have been described in *Stellarator News*, issues 15 and 23.

Island divertor

The second concept utilizes the existence of large magnetic islands at the plasma boundary; in the standard Helias configuration that is envisaged for Wendelstein 7-X five islands exist at the boundary with $\iota = 1$. Increasing ι to 5/4 at the edge yields four islands which usually are larger than those at $\iota = 1$. The X-point of these islands provides the diversion of the field lines and takes over the role of the helical X-line in torsatrons or in tokamaks. Streaming along the field lines, the plasma crosses the X-point region of the islands and arrives at the rear of the island after four to five toroidal transits.

Target plates are located in those regions where the plasma has reached the maximum distance from the main plasma after three to four toroidal transits. The islands and the X-line helically encircle the plasma column, and this configuration also forces the target plates to follow this geometry. The target plates are located in regions of minimum separatrix angle, gamma, since at these locations the out-streaming plasma is at the maximum distance from the main plasma (see the article in *Stellarator News* 15 by F. Hermegger). Small changes of the magnetic field by internal or external perturbations may ergodize the islands, but this does not spoil the divertor action as long as the position of the O-points stays fixed.

The viability of the island divertor concept depends on the stability of the islands against external and internal magnetic field perturbations and the capability to guide the outflowing plasma on target plates behind the islands. Several studies have been made to check this concept and to optimize the geometry of the target plates. These are

- Studies of the magnetic field structure, localization of the X-points and the O-points in the region outside the last magnetic surface, effect of perturbation fields on the islands, and geometry of flux bundles in the vicinity of islands;
- an investigation of particle diffusion in islands by mapping techniques and Monte Carlo techniques;
- a study of optimization of divertor target plates and the calculation of heat load on the target plates; and
- design of sweep coils for the control and modification of the edge fields, and for the reduction of the heat load by ac currents.

Target plates

The target plates are located on the top and bottom of the plasma column following the O-point of the $\iota = 1$ island, asymmetrically in the toroidal direction according to the helical geometry. The plasma flows across the separatrix of the island and meets the target plate on a narrow stripe.

Design criteria for the geometry of the target plates are as follows:

- The proposed target plates fit to various values of the rotational transform and permit a variation of the island size and position. In cases without islands at the boundary, the target plates act as limiters.

- ➡ The target plates are located in those regions where the islands have a maximum radial extent, which implies a large distance to the plasma.
- ➡ The shape of the target plates is designed such that a nearly constant intersection angle of the field lines at the highly loaded regions provides a smooth power load and avoids hot spots.
- ➡ The target plates have a toroidal length of 5 m, which is sufficient to keep the maximum power density within technical constraints. In addition, by use of the "shadow effect" leading edges are avoided (Fig. 1).

The proposed target plates are located on top and bottom, centered at the toroidal position of the bean-shaped plasma cross section at $\phi = 0$ (see Figs. 2 and 3). The problem arising from the different configurations created by variation of the rotational transform, ι, is solved by adjusting parts of the plates to each specific case. In the standard case [$\iota(a) = 1$] the field lines hit predominantly the center part of the plates; in the high- and low-iota cases [$\iota(a) = 5/4$ and $5/6$, respectively] the target plates are loaded more towards one or the other end.

For a given power flux along the field line, the intersection angle with the plates determines the power density. With an estimated width of the scrape-off layer (SOL) of about 2 cm and a heating power of 10 MW, an intersection angle of about 2 to 3° results if the power density is held below the technical limit of 10 MW/m^2. The total length of the plates, of about 5 m, is then determined by the intersection angle and the requirement that all field lines in the SOL hit the plates. In each of the five field periods, two target plates with an average width of 0.5 m are installed, resulting in a total surface of 25 m^2.

A Monte-Carlo technique is used to obtain the intersection patterns on the target plates, simulating the SOL by field-line tracing with perpendicular displacements (e.g., 0.1 cm for a diffusion coefficient $D = 1$ m^2/s) after each integration length of typically 30 cm. The starting points of the field lines are statistically distributed on a magnetic surface close to and inside the bounding separatrix; the integration is stopped at the target plates. There, the intersection points form stripes that are separated in the directions parallel or antiparallel to the magnetic field, where the separatrix and the adjacent field lines contact the target plates in a width reflecting the width of the SOL, as shown in Fig. 4. The intersection pattern on the target plates differs for the various cases examined:

Standard case (HS5V10N) — variation of $\iota(0)$ (0.83, 0.86, 0.89), variation of island size, variation of

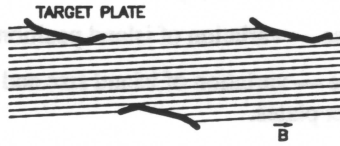

Fig. 1. Schematic arrangement of segmented target plates. Together with a nearly constant intersection angle the length of the target plates is chosen to protect the leading edge of each successive plate by the "shadow" of the previous one.

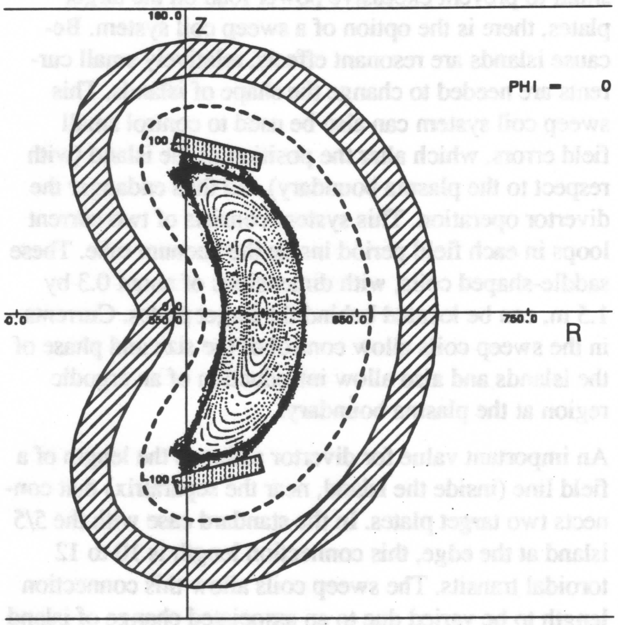

Fig. 2. Cross section of W7-X at the "bean-shaped" toroidal plane. Shown are the system of magnetic surfaces, the SOL represented by result of Monte-Carlo calculation, and the target plates. The first wall is shown as a dashed line and the radial dimension of the coil winding pack as the hatched area.

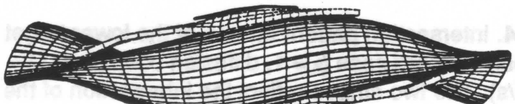

Fig. 3. Magnetic surface (one field period, just inside the SOL), target plates, and sweep coils of W7-X viewed from the radial outside.

island position, and variation of diffusion coefficient ($D = 1\ m^2/s$ and $0.2\ m^2/s$).

High iota case — variation of island position.

Low iota case — variation of island size and position of the target plates.

The stripes are narrower if the diffusion coefficient is reduced, and because the SOL width depends on the connection length and this length on the island size, the width of the stripes decreases when the island size is increased. The smallest stripes and largest power densities are found in the high-iota case.

Sweep Coils

If the diffusive broadening of the scrape-off layer is too small to prevent excessive power load on the target plates, there is the option of a sweep coil system. Because islands are resonant effects, relatively small currents are needed to change the shape of islands. This sweep coil system can also be used to control small field errors, which alter the position of the island (with respect to the plasma boundary) and thus endanger the divertor operation. This system consists of two current loops in each field period inside the vacuum tube. These saddle-shaped coils, with dimensions of about 0.3 by 1.5 m, can be located behind the target plates. Currents in the sweep coils allow control of the size and phase of the islands and also allow introduction of an ergodic region at the plasma boundary.

An important value for divertor action is the length of a field line (inside the island, near the separatrix) that connects two target plates. In the standard case with the 5/5 island at the edge, this connection length is 10 to 12 toroidal transits. The sweep coils allow this connection length to be varied due to an associated change of island rotational transform when changing the island size. Feeding the upper and lower sweeping coils with currents of opposite direction keeps the island size constant and achieves a poloidal shift of the island location. Reverse currents of 20 kA shift the X-point about 6 cm poloidally on the target plates. A sweeping effect is introduced when energizing the coils by ac currents; the transient magnetic field of the sweep coils oscillates the strike points on the target plates. Only relatively small currents are necessary to obtain the desired shift of the strike points because the X-points are part of the equilibrium field and need not be generated by the sweep coils.

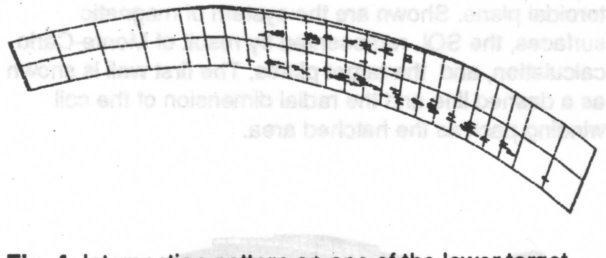

Fig. 4. Intersection pattern on one of the lower target plates, standard case ($\iota = 1$, diffusion coefficient $D = 1\ m^2/s$). The two stripes reflect the intersection of the separatrix with the target plates broadened by the diffusion. The separation in the directions parallel and antiparallel to the magnetic field is a consequence of the "shadow" effect.

A further application of the sweep coil system is the compensation of symmetry-breaking error fields, e.g., due to small construction inaccuracies of the device. Error field compensation is achieved by an individual choice of current in each sweep coil.

REFERENCES

[1] J. Nührenberg, R. Zille, Phys. Letters A **114**, 129 (1986).

Horst Wobig
Phone: 049-89-3299-1907
and Johann Kisslinger
Phone: 049-89-3299-1232
FAX: 049-89-3299-2579

Max Planck Institut für Plasmaphysik
Experimental Division E2
D-8046 Garching bei München, Germany